JOURNAL OF GEOPHYSICAL RESEARCH, VOL. 104, NO. B2, PAGES 2855–2874, FEBRUARY 10, 1999

Vertical movements and material transport during hotspot activity: Seismic reflection profiling offshore La Réunion

Béatrice de Voogd,[1] Salvador Pou Palomé,[1] Alfred Hirn,[2] Philippe Charvis,[3] Josep Gallart,[4] Dominique Rousset,[1] Juanjo Dañobeitia,[4] and Hervé Perroud[1]

Abstract. The structure of the submerged part of the La Réunion hotspot island is determined by a grid of multichannel seismic reflection profiles. The submarine part of the edifice appears as a poorly stratified wedge of material lying above a significant thickness of preexisting sediments and the oceanic basement. The dense data coverage has allowed us to derive contour maps of the top of the basement and of the base of the volcaniclastic edifice, further constrained by coincident wide-angle profiles. The resulting isobath maps reveal new, unsuspected features that could not be deduced from observation along a single seismic line since the geometry of these horizons varies significantly from one radial profile to the next. Both maps show a large degree of heterogeneity in the topography, with no axial nor cylindrical symmetry, indicating that plate flexure is not dominant. A slight depression toward the island is observed only in the southern area, ahead of the hotspot trace. The lack of angular unconformity in the volcano-sedimentary pile that covers the oceanic basement firmly establishes the lack of significant vertical movement and flexure. The base of the edifice is roughly domed, centered on the island, with several topographic highs or lows superimposed. The submarine apron appears as a composite constructional body, spreading by slumping of its flanks. Superficial lenses of laterally transported material are observed on the seismic data south of the island, not only to the east of the active Piton de la Fournaise volcano. Oceanic sediments trapped beneath the apron seem undeformed.

1. Introduction

Intraplate volcanism in oceanic regions is a topic of broad interest with implications going from deep mantle processes to surface natural hazards. Our understanding of moderate size volcanic edifices and related hotspot activity is essentially based on studies of the Hawaiian chain [*Watts et al.*, 1985; *Rees et al.*, 1993] and Marquesas archipelago [*Wolfe et al.*, 1994]. In this paper we present new deep seismic reflection data that reveal the three-dimensional structure of La Réunion, an active volcanic island which will be seen to exhibit peculiarities when compared to the Hawaiian analogue.

La Réunion is thought to be the most recent expression of an active hotspot in the western Indian Ocean [*Duncan et al.*, 1989]. The preexisting oceanic plate is of Paleocene age and was accreted through a complex pattern of seafloor spreading (Figure 1) [*Schlich et al.*, 1990; *Dyment*, 1991]. The hotspot track is outlined by the southern Mascarene Ridge and Mauritius Island. It is associated with a long-wavelength (1000 km) bathymetric high and a geoid swell [*Bonneville et al.*, 1988].

Previous studies, based on detailed bathymetric data, sonar images, sea bottom photographs, dredging, and coring, have provided evidence that lavas produced subaerially constitute the submarine apron of the eastern flank of the Piton de la Fournaise volcano [*Cochonat et al.*, 1990; *Lénat et al.*, 1990; *Labazuy*, 1991]. Thus landslides appear as a major volcano mass wasting process, as described in Hawaii [*Moore et al.*, 1989] or Tenerife [*Watts and Masson*, 1995]. However, until the survey we present here was performed, no data were available on the internal structure of the submarine edifice nor on its substratum.

[1]Laboratoire de Géophysique et UMR 5831, Université de Pau et des Pays de l'Adour, Pau, France.

[2]Institut de Physique du Globe de Paris, Laboratoire de Sismologie Expérimentale, UA 195 CNRS, Paris.

[3]Unité Mixte de Recherche Géosciences Azur, Institut Français de Recherche Scientifique pour le Développement en Coopération, Villefranche-sur-mer, France.

[4]Institut de Ciences de la Terra, Consejo Superior de Investigaciones Cientificas, Barcelona, Spain.

Paper number 98JB02842.
0148-0227/99/98JB02842$09.00

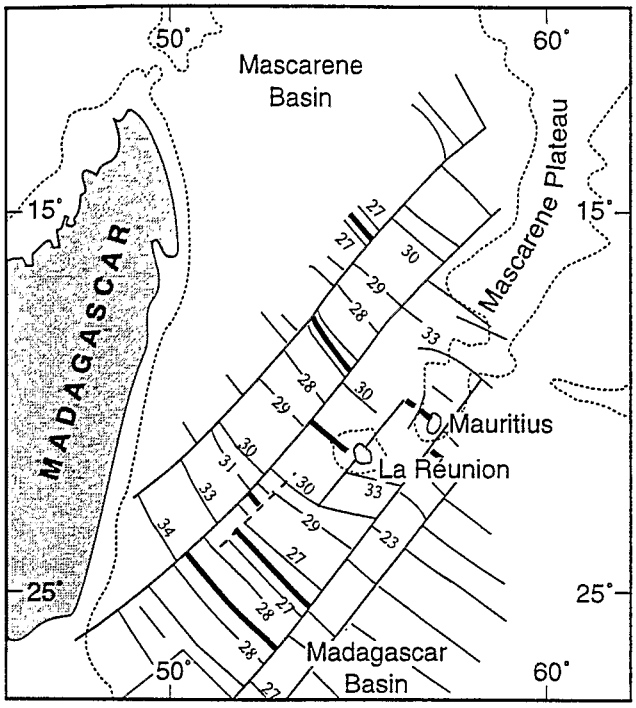

Figure 1. Location of La Réunion on the oceanic magnetic anomaly map adapted from *Dyment* [1991]; thick solid lines are extinct spreading centers; some magnetic anomalies are labeled, and fracture zones are sketched by thinner lines. Dotted line is the 3000 m bathymetric contour, drawn to outline major topographic features.

To assess the relation between intrusion, effusion, and lateral transport by tectonics and gravity, about 2500 km of multichannel seismic reflection (MCS) profiles were recorded during the REUSIS (Reunion Seismic) cruise made by the M/V *Marion Dufresne* (cruise MD-76) (Figure 2). These profiles straddle bathymetric features previously mapped by multibeam sounding [*Labazuy*, 1991], and several lines radiating from the island extend into deep water areas. The recording of coincident ocean bottom seismometers (OBSs) and MCS profiles provides additional constraints on velocity models, depth sections, and geological interpretation. In order to recognize the degree of relation of structural style with the presently active Piton de la Fournaise volcano, the survey was not restricted to the eastern side of the island. The density of seismic profiles (Figure 2) allows us to discuss the significance of radial variations at short wavelengths by comparing two nearby lines. Another objective was to test possible larger spatial wavelength changes of the structural variation radial to the island, when this radial goes from the direction towards the supposed hotspot trace (the northeast), through normal to it (the southeast), to away from it (the southwest).

A lithospheric transect along the trace of the La Réunion hotspot is presented by *Gallart et al.* [this issue]. In this paper, we use the grid of seismic reflection data to derive contour maps of the top of oceanic basement and of the base of the volcaniclastic edifice. These maps reveal unexpected topography, with no cylindrical nor axial symmetry, and are used to discuss vertical movements linked to hotspot discharge and evolution. The seismic profiles also provide new constraints on the mass wasting processes affecting the evolution of the volcanic edifice. Deep crustal and upper mantle magmatic processes are discussed on the basis of the wide-angle data [*Charvis et al.*, this issue].

2. Multichannel Seismic Reflection Data

2.1. Acquisition

Two kinds of marine seismic sources were used. A first set of profiles was recorded with an array of 6 x 9 L air guns equipped with a wave shape kit supposed to attenuate bubble oscillation [see, e.g., *Safar*, 1976a]; shot spacing was 50 m, resulting in 24-fold common midpoint (CMP) coverage with the 96-channel, 2400 m long streamer. This first part of the experiment was designed to obtain better resolution within the volcano-sedimentary pile near the Piton de la Fournaise. In the second part, a powerful source of 8 x 16 L air guns was shot every 80 s (shot spacing about 200 m, sixfold CMP coverage). This second series of profiles turned out to be equally useful to resolve internal structures of the volcanic edifice due to the successful prestack deconvolution described hereafter. Radial lines are numbered R1 to R23, with a w after the number if recorded with the 50 m shot spacing; other profiles (cross lines or circular profiles) are called C1 to C11 (or C*w if 24-fold). Data were recorded at 4 ms sampling rate; listening time was 18 s for the 24-fold profiles and 36 s for the others. The MCS shots were also recorded on OBSs and land stations (Figure 2).

All seismic reflection profiles were first processed on board to give brute stack sections. Gross features of the volcanic edifice can be interpreted on these sections, but poststack processing appears insufficient to interpret the various reflections ubiquitous in the volcano-sedimentary pile and to precisely delineate the top of oceanic basement, as illustrated by comparison of Figures 3a and 3b. This is essentially due to the long duration and relatively low frequency source signal of both arrays. Therefore a first task was to design an efficient prestack deconvolution and then to reprocess all the data. Only processing steps fundamental for data interpretation are discussed below.

2.2. Prestack Processing

Theoretically, the far-field source signature can be estimated from near-field measurements [*Ziolkowski et al.*, 1982; *Parkes et al.*, 1984]. Each gun was equipped with a near-field hydrophone, but most of them ceased to work as soon as the guns were put in the water, which meant that it would be impossible to follow the procedure described by *Ziolkowski* [1987]. However, our towing arrangement was such that this near-field partial recording could actually be used for designing a source signature deconvolution filter.

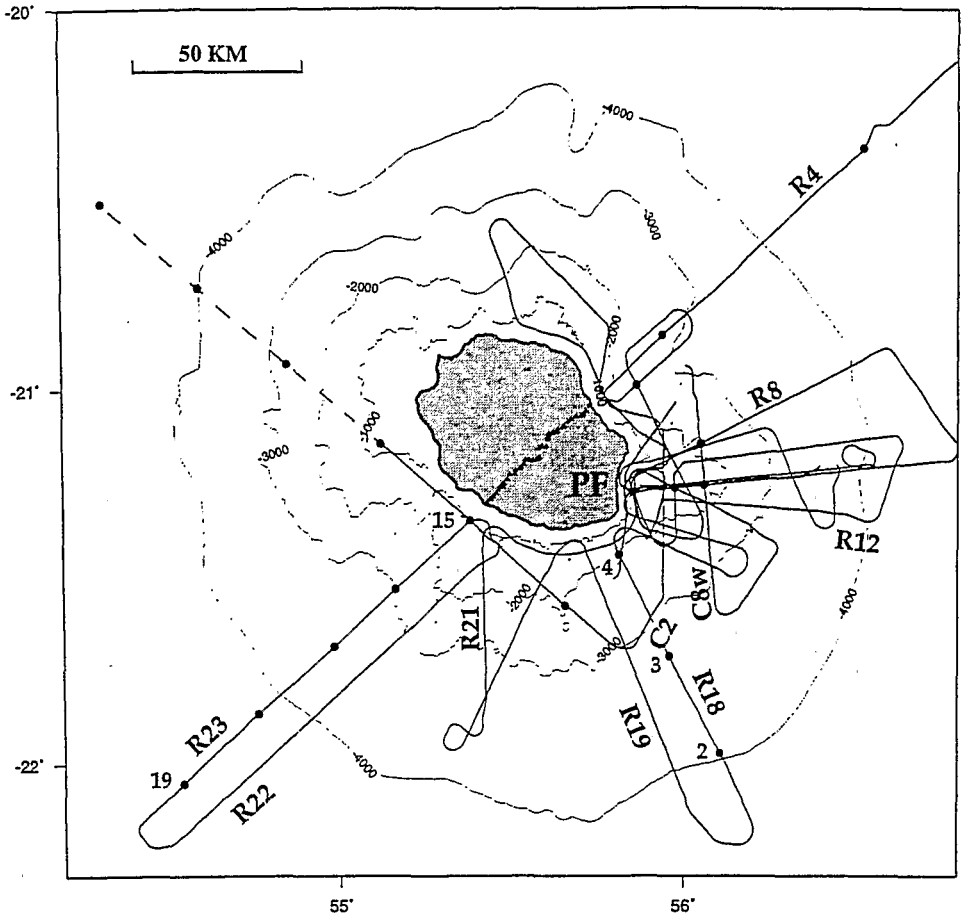

Figure 2. Location map of all multichannel seismic profiles (solid lines) recorded during the REUSIS (Reunion Seismic) cruise. Labels refer to profiles quoted in text. La Réunion is shaded; PF is the Piton de la Fournaise active volcano; bathymetry, contoured every 1000 m, is taken from *Labazuy* [1991]. Dots are ocean bottom seismometer (OBS) locations [*Charvis et al.*, this issue], numbered if mentioned in text or figures; dashed profile was only recorded on OBSs due to bad weather. Triangles are the land stations that recorded the main southwest-northeast transect (discussed by *Gallart et al.* [this issue]). A more detailed map of the eastern side of the island is provided in Figure 11.

The far-field signature of the source array is governed by the interaction between the guns and by the free surface effect (reflection at the surface of the water). The towing arrangement was of two identical subarrays, each on a string separated by a distance of about 28 m. On each string, the four guns were placed at 10 m intervals. Gun depth was estimated to be between 15 and 20 m, which gives a radius for the air bubble at equilibrium of less than 60 cm [*Safar*, 1976a]. Therefore mutual interaction between oscillating air bubbles was neglected despite the arguments developed by *Ziolkowski et al.* [1982]. The free surface effect can be calculated from near-field measurements if the gun depth is known [*Safar*, 1976b]. Here the first notch in the far-field signature amplitude spectrum is around 40 to 50 Hz, which is outside the frequency range of interest for us. The effect of the gun array is then approximately the sum of the effect of each single gun. Hence traces of each shot were deconvolved by the sum of the near-field recordings averaged for about 50 shots centered on that shot. Since it is likely that all guns did not tow at the same depth, this signature deconvolution cannot be perfect without near-field recordings of all the guns (nor without knowing exact gun depths), but results are quite good as confirmed by comparison of autocorrelations before and after deconvolution. The approach chosen is somewhat ad hoc but has its merit in the absence of proper knowledge of the far-field source signature. The data were then resampled at 8 ms. A classical predictive deconvolution was applied to complete the job and to attenuate the receiver ghost (i.e., reflection) from the free surface. Figure 4 summarizes these different steps and their effect on the data. This prestack processing, applied to all the data, benefits subsequent processing steps, in particular, velocity analysis.

2.3. Velocities

With a streamer of 2400 m and a fold of 6 for the CMP coverage of most profiles, little can be said about the velocities from the reflection seismic data alone,

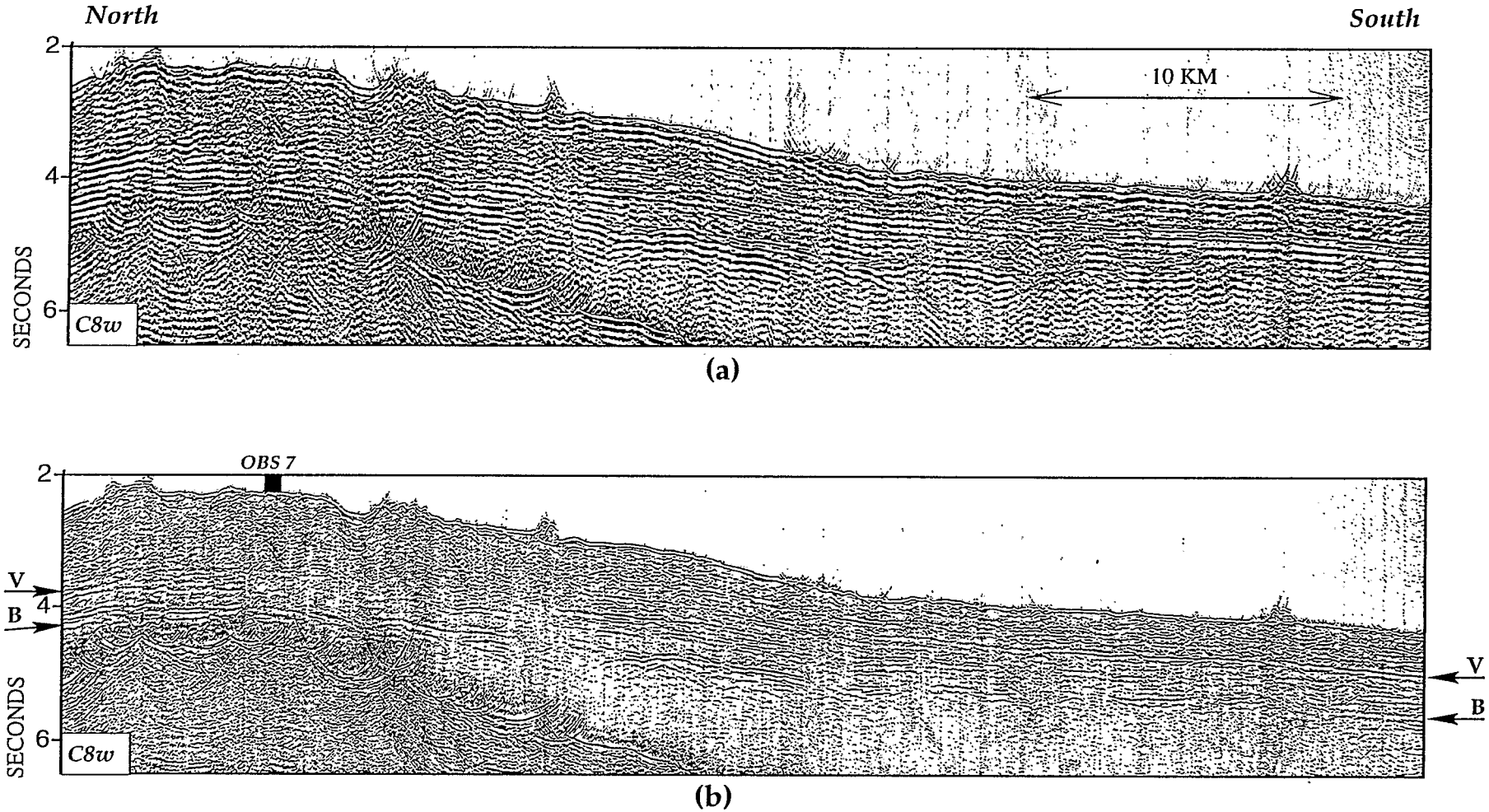

Figure 3. Part of profile C8w shown with migration in the frequency-wavenumber domain (fk) at a constant velocity of 1500 m/s applied after stack (a) without prestack deconvolution and (b) with signature deconvolution followed by predictive deconvolution before stack. V is the base of the volcaniclastic edifice; B is the top of oceanic basement. Note the thinning of the preexisting sediments (unit between V and B) on the basement high and the reverse polarity of V in the southern part of the profile.

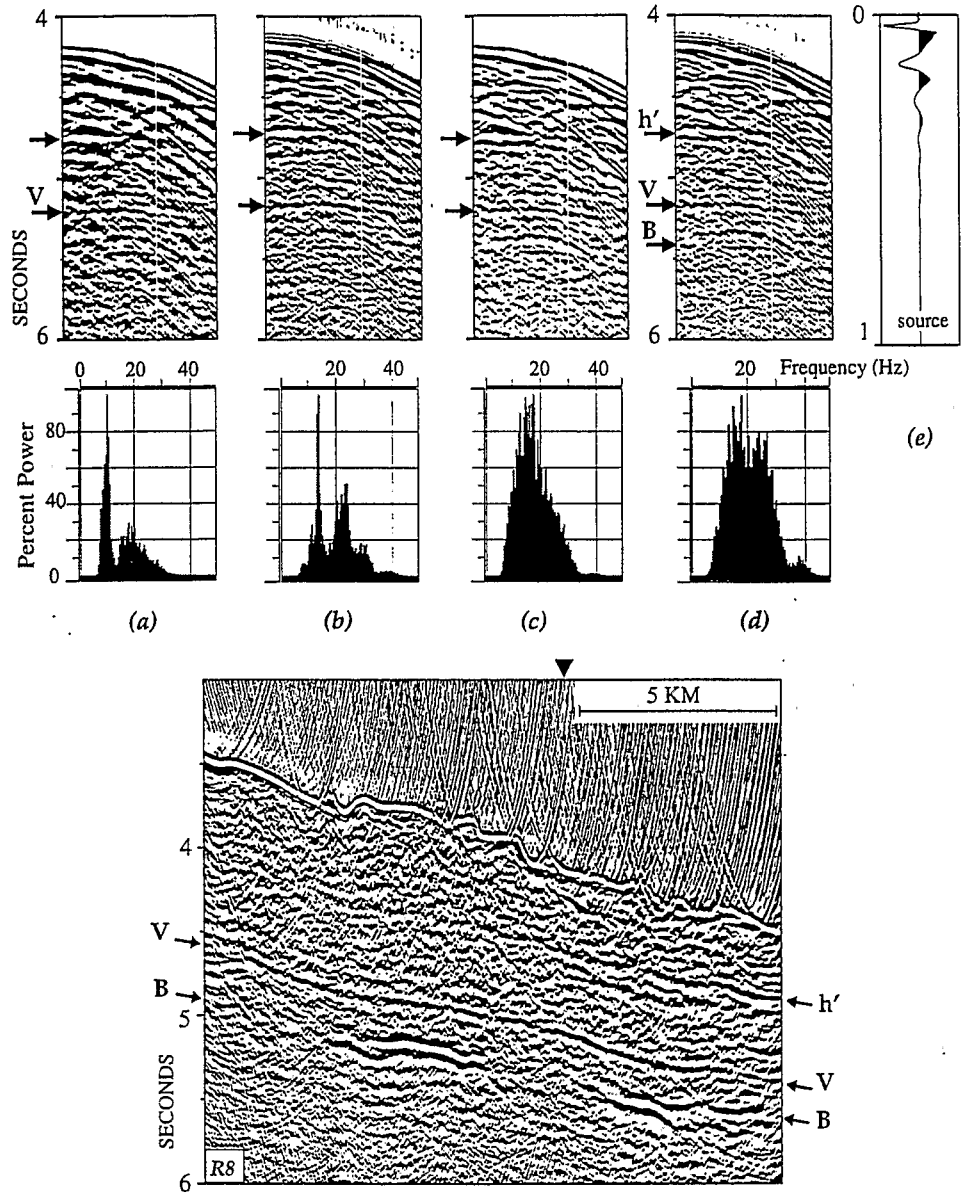

Figure 4. (top) A shot gather from the stack section illustrated below and corresponding frequency content (calculated between 4 and 6 s); h' is an intraedifice reflector, possibly the same stratigraphic horizon as reflector h, discussed in text; V is the base of the volcaniclastic edifice; B is the top of oceanic basement. (a) Raw shot gather. (b) Same shot gather as in Figure 4a after signature deconvolution using the source shown in Figure 4e. (c) Same shot gather as in Figure 4a with only predictive deconvolution applied. (d) Same shot gather as in Figure 4a after signature deconvolution followed by predictive deconvolution. (e) Source signature used for signature deconvolution in Figure 4b. (bottom) Time section of profile R8 with signature deconvolution followed by predictive deconvolution before stack and fk migration at a constant velocity of 1500 m/s after stack; the triangle on top indicates the location of the shot illustrated above (the ship was moving away from the island). Note the reverse polarity of V when compared to the seafloor reflection or to B.

especially in deep-water areas. However, a few inferences can be made from the 24-fold profiles and from analyses of "super gather" of the sixfold profiles (several adjacent CMPs merged together). Stacking velocities were picked interactively using simultaneously semblance analyses, unstacked CMP gathers, and constant velocity stack sections. In places where coherent subparallel reflectors are observed, interval velocities calculated from the stacking velocities were noted, and these values are used for the interpretation and comparison with the OBS results.

The most important and consistent result of this analysis is that interval velocities of the units mapped above oceanic basement do not vary significantly, being

around 4 km/s (±0.4), except for a few thin, superficial lenses with somewhat lower velocities (around 3 km/s). Velocities inferred from the wide-angle data are always within the range 3.5-4.5 km/s in the volcanic pile [*Charvis et al.*, this issue; *Gallart et al.*, this issue]. Average velocities around 4 km/s have also been reported for the Hawaiian [*Rees et al.*, 1993] and Marquesas [*Wolfe et al.*, 1994] aprons.

Several reflectors are observed between the seafloor and the top of oceanic basement. One of them, labeled V and hereafter interpreted as the base of the volcaniclastic edifice, has received much attention, leading to the following conclusions: Horizon V is never associated with a measurable change in interval velocity; if anything, a slightly lower velocity in the underlying unit could be documented on a few profiles, for example, in the southernmost portion of profile C8w (Figure 3) [*Pou Palomé*, 1997]. In several places, the reverse polarity of V, when compared to the sea bottom reflection, supports a velocity or a density inversion (Figures 3 and 4). Unfortunately, this could not be confirmed by the OBSs data since reflector V lies within a shadow zone. To fit both travel times and amplitudes of the wide-angle data, *Charvis et al.* [this issue] introduced a constant velocity layer beneath an upper unit with a positive velocity gradient; V lies within this constant velocity layer. They show that a velocity inversion coinciding with V can be introduced but its value is poorly constrained.

2.4. Migration and Depth Sections

Most profiles are plagued by arrivals scattered from the sea bottom or shallow inhomogeneities. These energetic events appear as easily recognizable diffraction hyperbolae on both shot point gathers and stacked sections but most often correspond to nearly flat normal-move-out curves on the CMP gathers. Therefore they cannot be attenuated by standard stacking procedures, especially when they come from out of the plane of section [*Larner et al.*, 1983; *Kent et al.*, 1996]. A simple poststack migration at 1500 m/s is quite useful to quickly remove most of the noise introduced by the small-scale seafloor topography.

More sophisticated migration schemes have been attempted. Dip move-out or other prestack migration schemes are hindered by spatial aliasing resulting from the 200 m shot spacing. Figure 5 shows an example of a finite difference depth migration (after stack); the resulting depth section provides a clear image of shallow structures, but for most of this study we prefer to discuss data interpretation on time-migrated sections without introducing poorly constrained small-scale lateral velocity variations in the volcanic apron.

Except for diffracted arrivals, the seismic sections show very gentle dips so the effect of migration is essentially to reduce diffractions from small-scale structures, while reflector geometry, on time-migrated sections, is not very sensitive to the velocity model used for migration.

The cause of apparent reflector geometry is essentially bathymetric variation. Since the volcano-sedimentary pile that overlies igneous basement has a fairly constant average velocity of about 4000 m/s, we have constructed pseudo-depth sections by converting time sections into depth, taking a velocity of 1500 m/s in the water and a uniform velocity of 4000 m/s below sea bottom. As a result, topography of the various seismic horizons is closer to reality, having been corrected

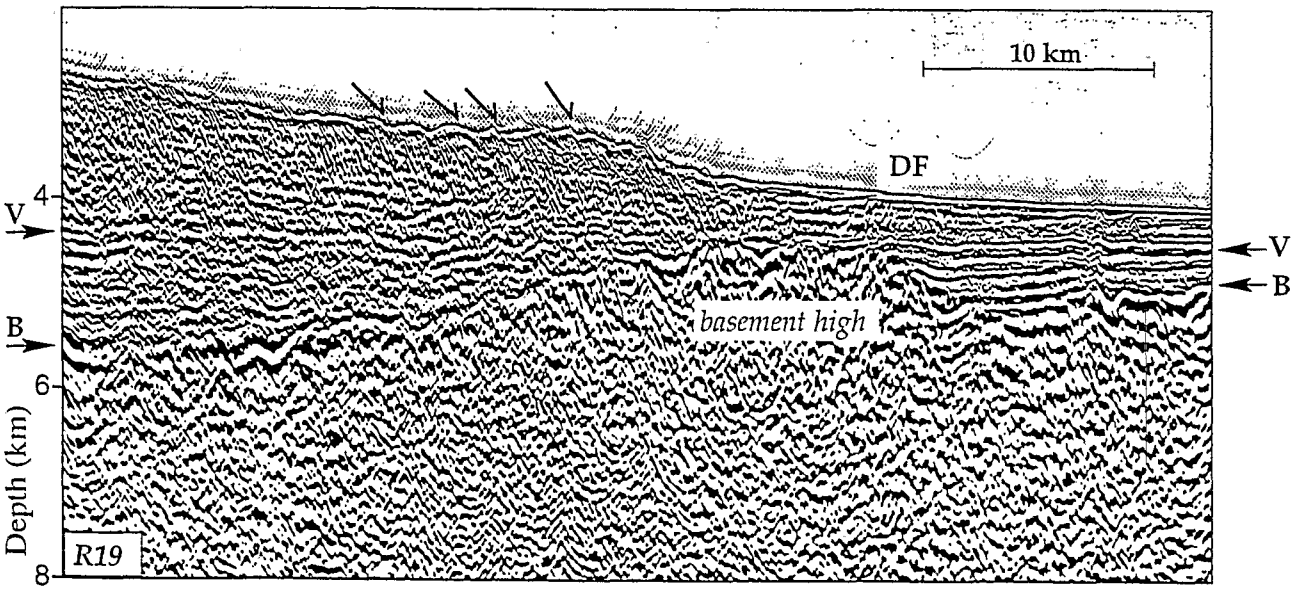

Figure 5. Finite difference depth migration of central portion of profile R19; see Figures 2 and 6 for location. V is the base of the volcaniclastic edifice; B is the top of oceanic basement. Half arrows indicate examples of the normal faults mentioned in the text. DF marks the outer limit of observable deformation in the apron.

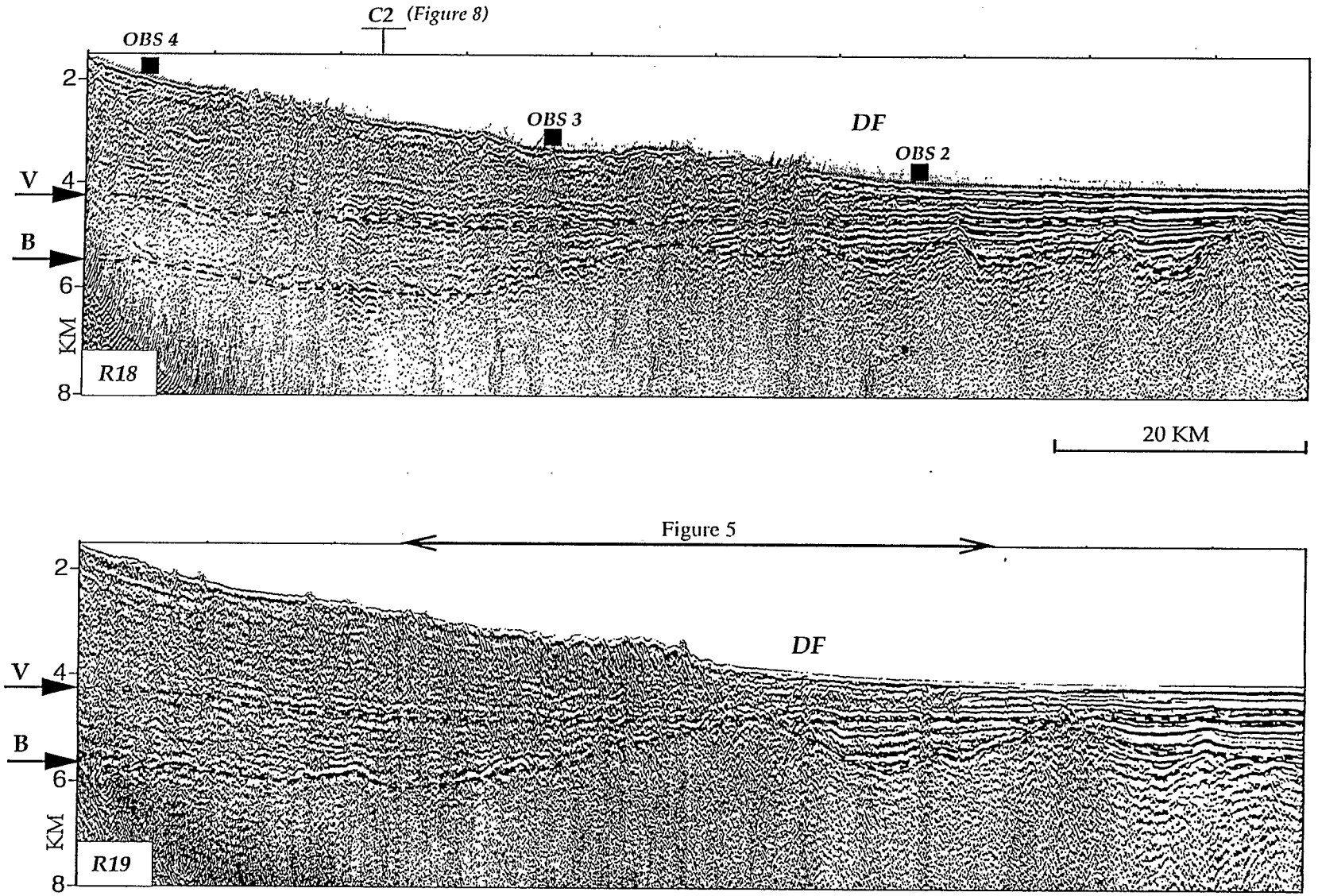

Figure 6. Pseudo depth sections of profiles (top) R18 and (bottom) R19. These are time-migrated sections converted to depth with a simple velocity model (1.5 km/s in water, 4 km/s underneath) to correct for bathymetry. V is the base of the volcaniclastic edifice; B is the top of oceanic basement. Note the variation in oceanic basement topography between these two nearby radial profiles (see Figure 2 for location).

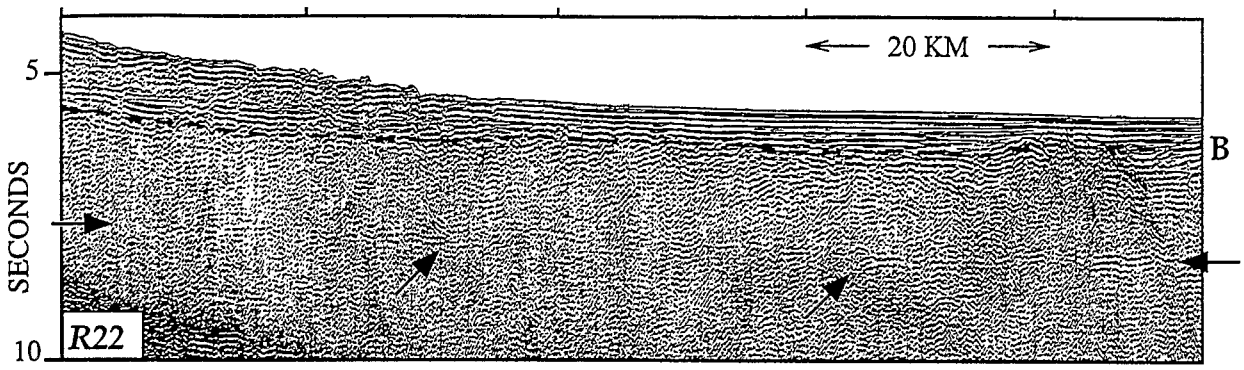

Figure 7. Brute stack of profile R22 where a continuous reflection from the base of the crust (arrows) is observed. Such deep events are best seen on the brute stacks since parameters for prestack deconvolution were picked to improve the upper part of the sections. The top of oceanic basement is labeled B.

from the deformation (velocity pull up or down) due to the dip of the sea bottom. The resulting sections (e.g., Figure 6) can therefore be thought of as time sections corrected for bathymetry but with a variably stretched vertical scale below sea bottom. They are useful to illustrate large-scale features, though detailed picking of reflections was done on time sections. Comparison of Figures 5 and 6 illustrates that reflectors dips are gentle enough to validate our approach.

2.5. General Features of the Seismic Sections

For brevity, the MCS profiles are described in terms which reflect our preferred interpretation, discussed here. All seismic lines show series of reflectors between the sea bottom and the acoustic basement, labeled B on figures, and interpreted as the top of the oceanic basement. These reflectors define several units of variable thicknesses and lateral extents. Two major units are distinguished and correlated on all profiles. The boundary between these units is labeled V on figures. The upper sequence is interpreted as the volcaniclastic edifice and the lower one as the preexisting oceanic sediments.

What we call the volcaniclastic edifice includes everything that was deposited on the preexisting oceanic crust since the onset of La Réunion volcanism, at least 2.1 m.y. ago for subaerial activity [*McDougall,* 1971], regardless of the processes involved (lava flows, mass wasting from the upper part of the edifice, sedimentation). That may also include units intruded within the apron itself, though this last point cannot be documented by our data.

No convincing intrabasement features are observed, except for a relatively continuous arrival that can be traced along several of the reflection profiles at an almost constant time of about 8 s in deep-water areas (Figure 7). It correlates with the base of the crust as determined from the OBS data.

The radial lines exhibit some common features but also show significant variations in the uppermost structures. For example, the two radial profiles illustrated in Figure 6, though only 10 km apart (Figure 2), show significant differences in bathymetry, shape and structure of the volcaniclastic edifice, and topography of the top of oceanic basement. It is therefore not possible to draw conclusions about the structure of the edifice from a single transect, and we shall now describe isobath maps derived from the synthesis of all seismic profiles. A detailed description of the MCS data is given by *Pou Palomé* [1997].

3. Mapping the Volcaniclastic Apron and Its Substratum

The top of the igneous basement is a marker of the accretion history of the oceanic crust. It is also the only horizon that we can interpret without ambiguity on both the MCS and the OBS data. In other areas, it has been used as a marker of the plate flexure linked to the load of islands [e.g., *Watts et al.*, 1985]. At La Réunion, because of the presence of a significant thickness of preexisting oceanic sediments, we can also map the base of the volcanic edifice as a distinct horizon; this horizon is the top of the preexisting oceanic plate.

3.1. Topography of the Top of the Igneous Basement

The top of the oceanic basement, labeled B on figures, is well defined by the reflection data, even beneath the thickest parts of the edifice or through the water bottom multiple. It is either a strong, continuous reflector or the envelope of diffraction hyperbolae associated with rough igneous basement. It was systematically digitized on the MCS sections. Depth conversion was calculated with a constant velocity of 4 km/s beneath seafloor, and 1.5 km/s above. Results are summarized by the isobath map shown in the lower part of Plate 1 (bottom). This map has been smoothed and is intended for discussion of large-scale features. It is consistent with general features interpreted from the wide-angle data [*Charvis et al.*, this issue]. The major result is that the MCS survey

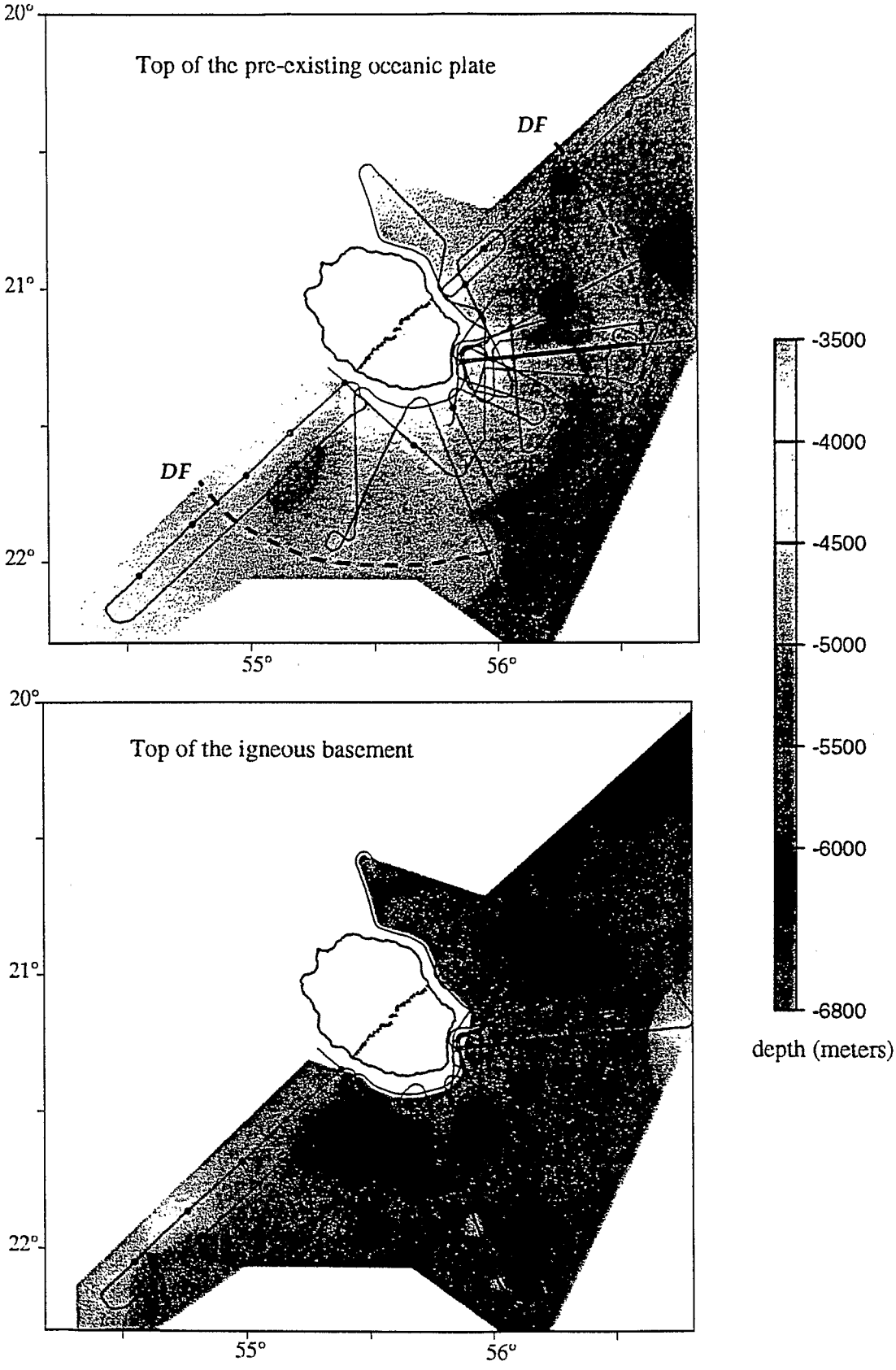

Plate 1. Isobath maps, in depth, (top) of the top of the preexisting oceanic plate, i.e., the base of the volcaniclastic edifice, and (bottom) of the top of the igneous basement; these horizons are labeled V and B, respectively, on the seismic sections; conversion velocity is 1500 m/s in water and 4000 m/s below. MCS profiles are drawn in thin solid line and indicate actual data points; large areas where no data are available are left blank. Specific features of these maps are discussed in text and illustrated by selected portions of the seismic profiles. On the top map, dashed line (DF) indicates the outer limit of the area where deformation of the edifice could be documented; it is used to calculate the volume of the edifice as discussed in the text. Note that

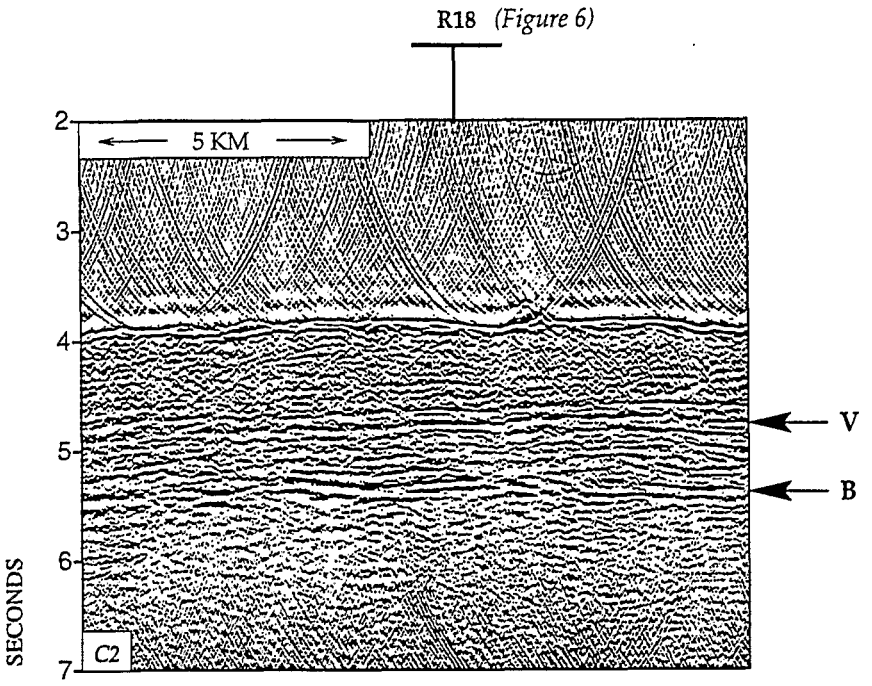

Figure 8. Part of profile C2 (deconvolved before stack and fk migrated at a constant velocity of 1500 m/s after stack) showing the contrast in seismic character between the volcanic edifice and the preexisting oceanic sediments. The top of oceanic basement is labeled B, and the base of the edifice is labeled V.

reveals significant three-dimensional (3 D) variation of the topography of the preexisting oceanic basement as a function of the direction to the island. Southwest of the island, profiles R22 and R23 document a slight deepening (1000 m at most) of the top of basement toward the island. The other radial profiles show either shallowing of the oceanic basement toward the island (northeastern side) or a complex topography with highs and lows.

The southeastern side of the island is bordered by a pronounced arcuate depression which is itself bordered by two basement highs, one outward and one along the shore (Figure 6 and Plate 1). This last one is further documented by the wide-angle data along profile R18 [*Charvis et al.*, this issue].

A basement high is observed east of the Piton de la Fournaise. Its trend, about N80°, is constrained by north-south profiles (e.g., Figure 3) and by profiles north and south of the radial profile R12 (located on Figure 2) that roughly follows this ridge. It is therefore not an artifact from inadequate sampling.

Additional complexity is evidenced by comparing nearby radial profiles. For example, R22 and R23, only 15 km apart and roughly parallel to the direction of seafloor spreading (Figure 1), indicate a rather abrupt change in depth to basement, attributed to the presence of a fracture zone between these profiles, as discussed in section 5. Farther to the east, and with a completely different orientation, profiles R18 and R19 also show significant variations in basement topography (Figure 6).

3.2. Topography of the Top of the Preexisting Oceanic Plate

Identifying the top of the preexisting oceanic plate (i.e., the base of the edifice) on the seismic profiles is not without ambiguity since several reflections could be considered as candidates for it. Our interpretation is based on the following criteria. First, and most importantly, we have used the fact that the 23 radial profiles are all connected by circular profiles or cross lines (Figure 2). All profile intersections were checked for consistency in interpretation. V is the only seismic horizon that can be correlated on all profiles, though it is not everywhere a continuous reflector, possibly due to wavefield distortion by near-surface topography or complex, small-scale heterogeneities along this inferred limit. Second, V is often taken as the boundary between units that can be distinguished on the basis of their seismic character (e.g., Figure 8). The reflective character of the lowermost unit, which lies directly on top of igneous basement, is attributed to the presence of oceanic sediments that predate the volcanic edifice. Third, V coincides with an unconformity on a few sections (Figures 5, 6, and 9). Other unconformities are observed within the apron (h, Figures 10 and 11), but they are stratigraphically younger than V, and their significance is discussed in section 4.2.

In summary, the approach used to construct the map illustrated on Plate 1 (top) is the following: Starting independently from several places where the position of V is unambiguous (for example, the unconformity

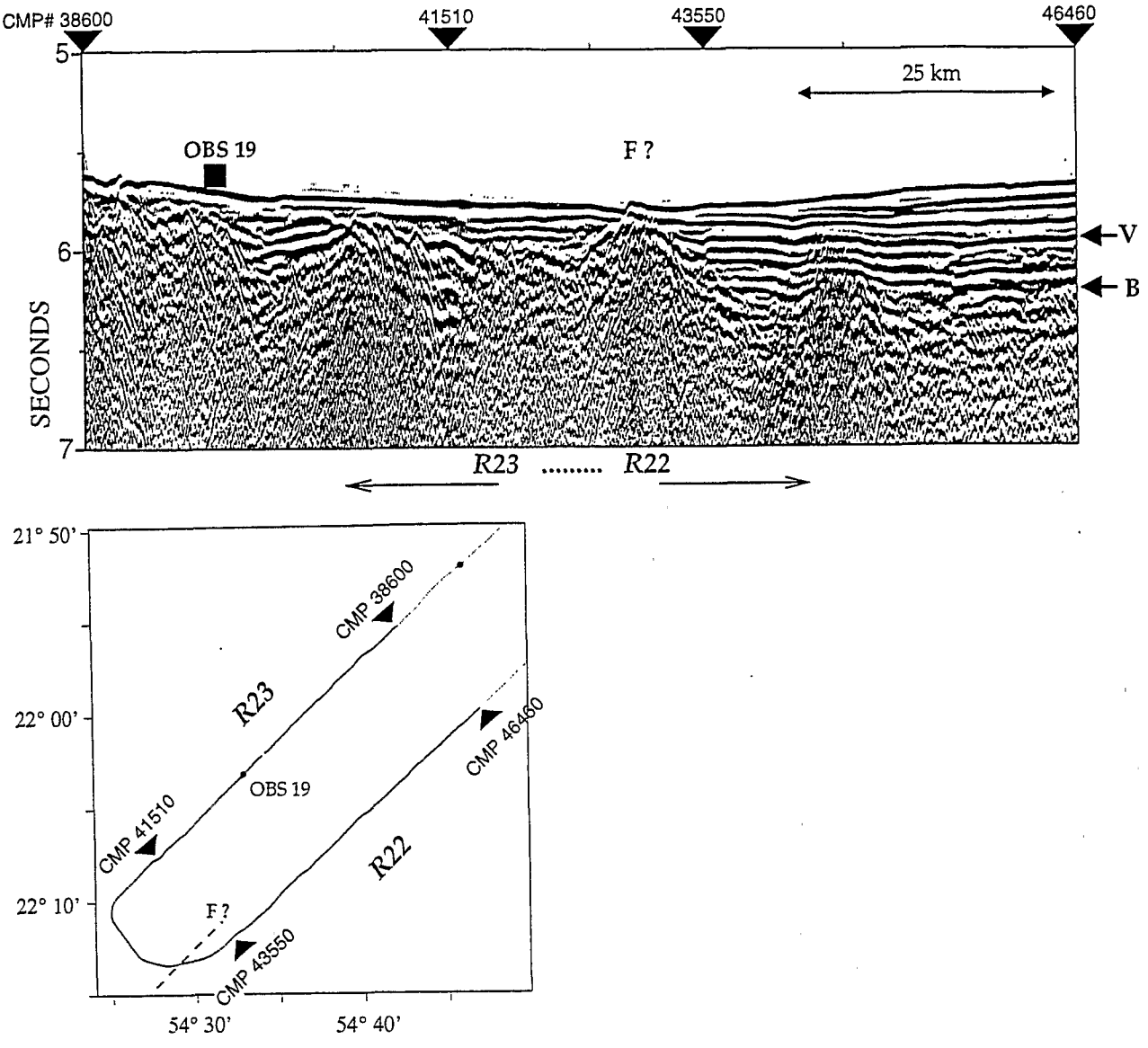

Figure 9. Migrated time section of the southwestern end of profiles R22 and R23 to illustrate that vertical movements linked to hotspot activity may reactivate older zones of weakness such as fracture zones. B is the top of oceanic basement. The difference in depth to basement between profiles R22 and R23 is one of the features apparent in Plate 1, southwest of the island; it may follow one of the fracture zones inferred by *Dyment* [1991] (Figure 1). F? is a recent fault scarp. The islandward stepping of reflector terminations observed in the uppermost sediments and the unconformity which is taken as the base of the volcaniclastic edifice (labeled V) suggest that the southeastern block moved upward.

shown in Figure 6 or 9), we traced V to line intersections. Working step by step, we produced a time pick of V consistent with all available data. The time horizon was then converted to depth with a constant velocity of 4 km/s below seafloor and 1.5 km/s above seafloor. With these criteria, V corresponds to a minimal edifice thickness. The choice of a constant velocity for the depth conversion will introduce artifacts if lateral velocity variations are present. One example may be the trough apparent on Plate 1 (top) southwest of the island and centered on profile R22; it correlates with a relative bathymetric high when compared with profile R23 at the same distance from the island (Figure 2). Introducing a lower-velocity unit in the superficial part of the edifice could suppress this apparent trough. However, the topographic high observed just east of the island (in bright orange on Plate 1), which also correlates with a bathymetric high, would only be exaggerated by the existence of a low-velocity unit above it.

Large-scale features of the maps of Plate 1 are constrained by the wide-angle data [*Charvis et al.*, this issue]. The major result of this study is that the top of the preexisting oceanic plate is not flexurally downwarped toward the island. It has a roughly domal shape. Noth-

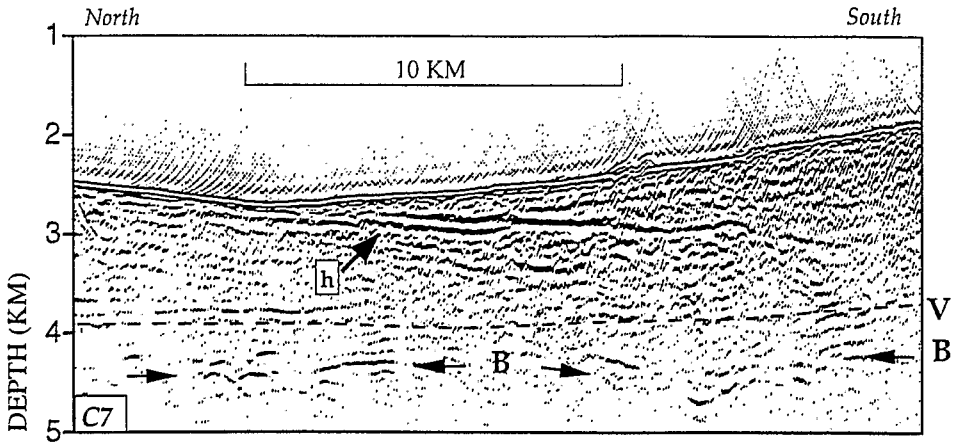

Figure 10. Small portion of profile C7 (see Figure 11) showing a distinctive unit, resting unconformably above an older part of the edifice. The unconformity which marks the base of this unit is labeled h. This unit can be mapped over an area of at least 200 km^2 east of the island (see Figure 11). V is the base of the volcaniclastic edifice; B is the top of oceanic basement. This is a time-migrated section converted to depth with a velocity of 3 km/s. Note that the wedge of volcaniclastic material appears to fill a preexisting depression of the volcanic apron. Taking a higher velocity for depth conversion increases this depression.

ing like the Hawaiian or Marquesas basement moat is observed.

3.3. Preexisting Oceanic Sediments

Our interpretation implies a relatively thick layer of sediments covering the Paleocene igneous basement (about 600 m in average, up to 1000 m above basement lows). Drilling on the Mascarene Plateau has provided evidence for a neritic platform just north of La Réunion in the early Tertiary [*Bassias et al.*, 1993]. In addition, Mauritius Island has been an important source of volcanogenic sediments for the past 7 or 8 m.y.. This is consistent with the observed overall increase in sediment thickness to the north of La Réunion.

Studying the preexisting sediments is informative in several respects. First, they can be used as stratigraphic markers of the timing of the deformation that produced the observed basement topography. Second, experimental models of volcanic spreading imply deformation within the substratum [*Merle and Borgia*, 1996]. This is not documented by our data; however, we cannot rule it out since it is impossible to distinguish between true structure and velocity pull up or pull down induced by the poorly constrained small-scale heterogeneity of the overlying apron.

3.4. Volume of the Edifice

With the stratigraphic definition of the volcaniclastic edifice used above, the outer edge of the edifice would be as far away as volcanogenic sediments could go. This is, of course, not a suitable definition of the structure of the edifice. Therefore, while keeping our definition of horizon V, based on seismic stratigraphy, we will define the outer edge of the edifice as the farthest evidence of deformation through mass wasting processes. This limit is called deformation front (DF) on the seismic sections and is shown as a dashed line on Plate 1. It roughly coincides with isobath 4000 m of the bathymetry, giving a diameter of about 200 km.

The isobath map of the base of the edifice (Plate 1) can now be used to give an estimate of the volume of the submarine apron of about 60,000 km^3. This was done by calculating the volume between horizon V and the seafloor in the area delimited by DF, the edge of the island, and radial profiles R4 and R23 (see Figure 2), and multiplying it by 2, assuming symmetry of the edifice. Of course, this estimate depends on the velocity model used to convert the time horizons into depth. The choice of a constant conversion velocity of 4 km/s will, if anything, tend to overestimate the volume, since lower-velocity units appear to be included in the upper part of the apron in a few places.

To discuss the load resulting from the edifice, the volume of the island itself must be added to the above number. This volume is the sum of the emerged part of the island (2300 km^3 calculated from the digital elevation model) and the part below sea level, about 12,000 km^3 from the wide-angle results [*Charvis et al.*, this issue], giving a total volume of about 75,000 km^3.

Our estimate is much less than previous ones (240,000 km^3 for *Lénat and Labazuy* [1990]) that included a 4 km flexural depression relative to the average depth to oceanic basement, which was found nonexistent by our survey. This volume of 75,000 km^3 is relatively small when compared to other oceanic volcanic islands but is consistent with the effusion rate of 0.01 km^3/yr proposed by *Lénat* [1987] and also reported by *Stieltjes and Moutou* [1989] over the period 1931-1985 if we assume that the 2 m.y. of known aerial volcanic activity has

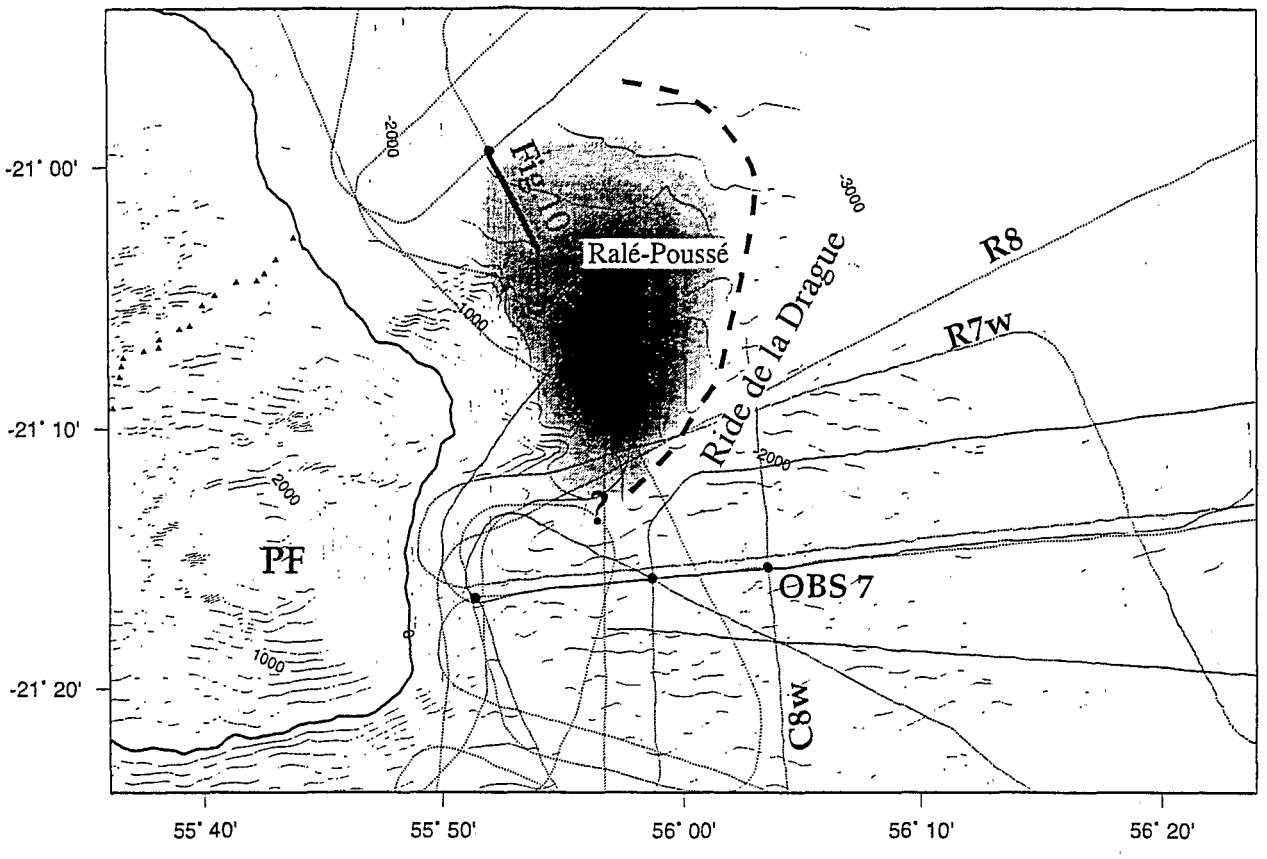

Figure 11. Isopach map of the unit above unconformity h, illustrated in Figure 10; white is zero thickness, darkest area is 1250 m thick; drawn here is the minimun extent of this unit, the bold dashed line indicating the area where we could not conclusively trace h and tie it to a similar feature called h' (Figure 12). Note that this unit is at least 5 times thicker than the one inferred by *Labazuy* [1991] on the basis of multibeam data. Here the velocity used for depth conversion was 3 km/s; taking a higher velocity for depth conversion increases the thickness of this unit. Thin solid line is bathymetry, drawn every 200 m and taken from *Labazuy* [1991]; thin dotted lines are MCS profiles; profiles mentioned in text are labeled.

been preceded by a few million years of submarine activity. This is quite reasonable since volcanism ceased on Mauritius Island 7 or 8 m.y. ago. A discussion of the relative volumes of intrusive and extrusive products is proposed by *Charvis et al.* [this issue] on the basis of the velocity structure interpreted from the wide-angle data.

4. Structure of the Submarine Edifice and Flank Instability

4.1. Structure of the Edifice

Several features, all with variable seismic character and lateral extent, are observed within the volcaniclastic edifice and used below to discuss its deformation and evolution: relatively thin and irregular superficial units (Figure 12), bathymetric bulges where the seafloor is chaotic (e.g., Ride de la Drague, Figure 13), extensional and compressional faults (Figures 5, 13, and 14), subhorizontal reflectors suggesting gliding planes or decollement surfaces (Figure 14), and wedges or lenses of material lying unconformably on top of older parts of the edifice (Figure 10). The terminology used here follows *Varnes* [1978].

The thin (<300 m) superficial units, such as the one illustrated Figure 12, are characterized by a smooth lower boundary contrasting with rugged seafloor. They are found predominantly near the island or downslope from bathymetric highs. We interpret them as the seismic expression of debris avalanches.

Superficial lenses and apparently thicker, chaotic zones (Figure 13) are not restricted to some areas such as the offshore of the active volcano, nor do they simply correlate there with units mapped by *Labazuy* [1991] on the basis of seafloor morphological studies. Bathymetric bulges are observed on most profiles. They occur downslope of relative lows in the bathymetry (e.g., Figures 5, 6, and 13). Their internal structure is poorly imaged, possibly because of intense, small-scale internal deformation. They are interpreted as zones of accumulated landslide deposits, associated with negative relief upslope.

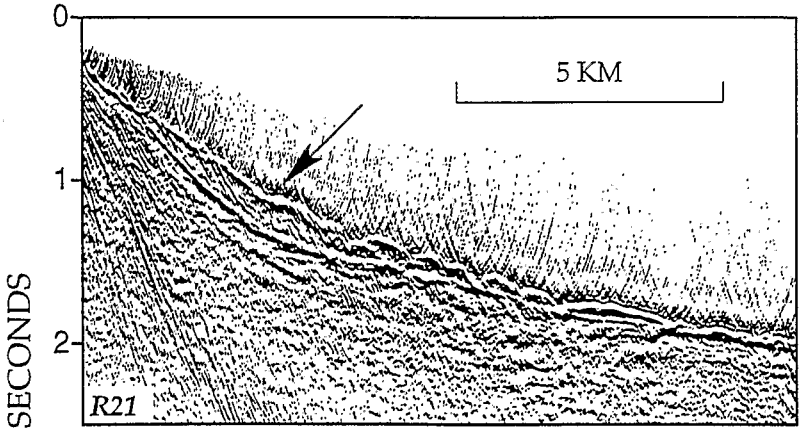

Figure 12. Northernmost portion of profile R21 (see Figure 2) to illustrate an inferred debris avalanche south of the island; this is a CMP-stacked section migrated at a constant velocity of 1500 m/s. The arrow points to a relatively thin unit of debris that is also imaged on intersecting lines to give a minimum volume of 10 km^3; near the arrow, thickness reaches about 250 m.

Geometrical relationship of shallow structures suggests the presence of both normal and reverse faults (Figures 5, 13, and 14) induced by slumping. At the head of each slump, a tensional depression is ubiquitous in the bathymetry; it is paired with compressional structures giving relative bathymetric highs farther downslope.

Strike-slip or transfer faults are difficult to document on the MCS data; they may exist and limit sectors of the collapsing volcanic edifice, though, as will be argued below, preexisting topography appears as the leading factor in controlling lateral transport.

Many reflectors are observed within the volcaniclastic pile, but their lateral extent is, in most cases, too limited to allow interpretation. Only a few can be imaged on intersecting profiles, ruling out side echos, but these reflectors appear to simply fade out. The observation of clear images from underlying horizons suggests that this is not a problem of seismic penetration. It could be that internal deformation of the uppermost layers is so intense that underlying reflectors loose their continuity and are not resolved by the MCS data. It may also be that the impedance contrast giving rise to the observed reflectivity is a localized phenomenon, linked, for example, to a thin layer of ashes, or pelagic sediments.

One reflector with an exceptional extent is found northeast of the island where, on several profiles and consistently at their crossing points, a clear arrival (labeled h on Figure 10) can be followed over a distance of at least 25 km. It forms the base of a layer of significantly lower interval velocity (about 3 km/s) above a substratum where average interval velocity is at least 4 km/s. This unit thins out, and its base almost reaches sea bottom at the northwestern end of profile C7 (Figure 10). Its eastern termination is not so clear. A similar feature, labeled h', is mapped in a zone just a few kilometers south (Figure 4). It is quite possible that h and h' correspond to the same stratigraphic horizon, but this cannot be ascertained since the reflectivity of both h and h' fades out at critical line intersections.

4.2. Landslide Processes, Internal Deformation, Construction, and Destruction of the Edifice

Several lines of evidence, summarized in the discussion, suggest that gravitational collapse rather than magma-driven edifice spreading is the primary cause of slope instability at La Réunion. Caldera collapse, slope failure, and catastrophic mass wasting events have been documented from surface geology [*Chevallier and Bachèlery*, 1981; *Duffield et al.*, 1982; *Gillot et al.*, 1994; *Bachèlery et al.*, 1996]. Previous studies based on multibeam sounding and sea-bottom photographs had led to recognition of lateral transport over distances of at least 30 km east of the island [*Lénat et al.*, 1990; *Labazuy*, 1991]. These last authors imaged superficial features that we cannot resolve with seismic profiling. The MCS data discussed here have a vertical resolution of 30 m, at best, for the upper layers, which explains why units mapped by *Labazuy* [1991] may not be seen on the MCS profiles. It is likely that units recognized on the seismic data encompass several structural units like the most recent of the ones mapped by *Labazuy* [1991]. A new result is that our survey documents the existence of slope instabilities south of the island (Figure 12), not only in relation with the active Piton de la Fournaise volcano.

Slope instability results in two categories of landslides, as has been described in Hawaii [*Moore et al.*, 1989, 1994]. Slumps refer to slow deformation of large areas of the edifice. Debris avalanches are catastrophic slope failures. The widespread occurrence of both mechanisms is suggested by our data. The seismic expression of the outer edge of the edifice (DF) and of bathymetric features located between the edge of the island and DF

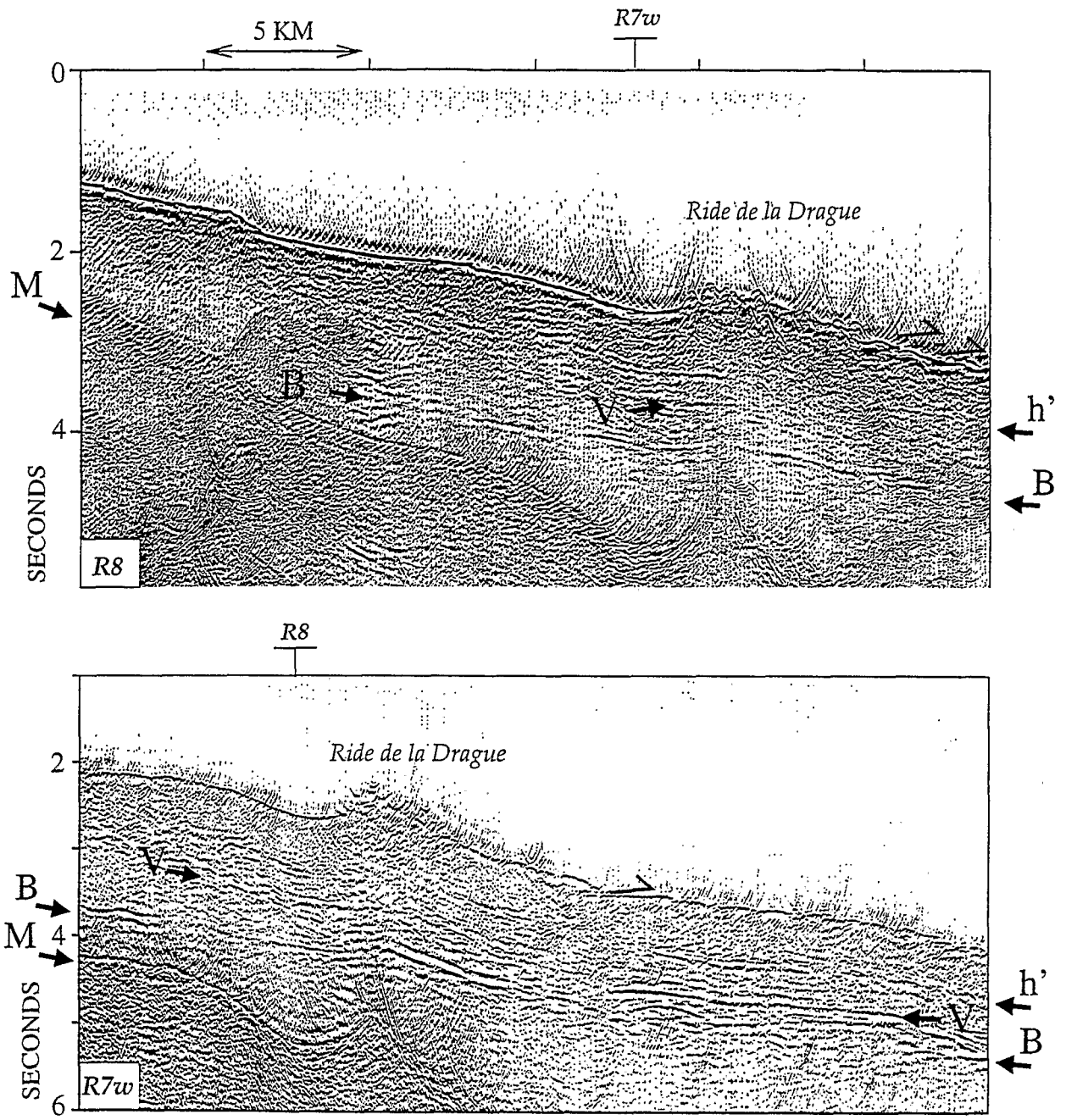

Figure 13. Portion of intersecting profiles (top) R8 and (bottom) R7w to illustrate mass wasting processes and deformation of the edifice; see Figure 11 for location. V is the base of the volcaniclastic edifice; B is the top of oceanic basement; h' is an intraedifice reflector; M is the first water bottom multiple. The bathymetric bulge known as the Ride de la Dragué is interpreted as a zone of accumulated landslide deposits. The half arrows outline reverse faults. The difference in seismic character is partly due to the different air gun sources used; processing for both profiles was identical, with signature and predictive deconvolution before stack, and fk migration at 1500 m/s after stack; scales are identical.

may be related to mass wasting processes. Avalanche flows undergo a size sorting of their constituting elements with distance and basically thin out and widen toward their distal part. In contrast, the outboard edge of a slump will not fade out but will form a toe over the preexisting downslope. This relief may in turn undergo normal faulting, as evidenced on profile R19 (Figures 5 and 6) where a marked bulge of deposits is observed to be severely deformed.

4.2.1. Nature of the failure surface. In Hawaii, geological, geodetic, and earthquake data suggest that seaward slip of the southern flank of Kilauea volcano is accommodated by a decollement located at the base of the volcanic pile [*Lipman et al.*, 1985; *Denlinger and*

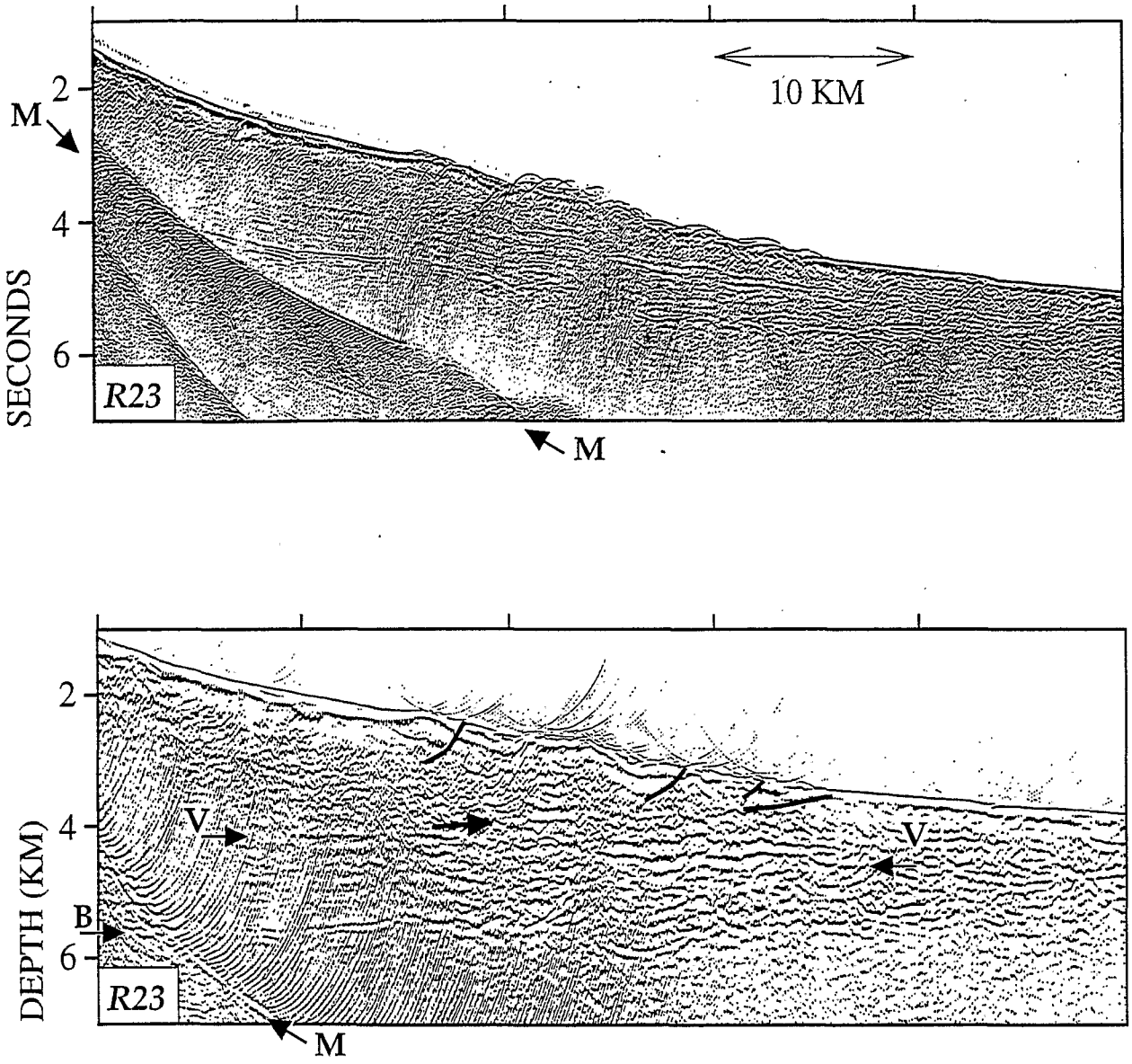

Figure 14. Portion of profile R23 (top) unmigrated and (bottom) migrated at a constant velocity of 2500 m/s and converted to depth; velocity used for depth conversion is 1500 m/s in the water and 4000 m/s below. The relatively low velocity used for migration minimizes artifacts; the point here being to discuss the maximum depth of deformation. Continuous lines indicate major faults. The unlabeled bold arrow, just above horizon V, points to a possible gliding plane mentioned in the text (dip ranges from 2 to 20°); these structures appear to root at the base of the edifice (horizon V).

Okubo, 1995; *Wallace and Delaney*, 1995]. At La Réunion, our seismic images are consistent with mechanical decoupling between the edifice and the preexisting sediments (Figure 14), though other, higher decollement levels and gliding planes are likely. On a few profiles, faults or gliding planes appear to affect the distal part of the whole volcanic edifice and may root into the boundary between the volcanic edifice and the preexisting oceanic sediments (Figure 14). Several levels of decollement, possibly correlated with edifice thickness, are therefore suggested by our data, but they never occur deeper than V.

A genetic relation may exist between localized bulges of the volcaniclastic edifice and location of oceanic basement highs (Figure 5). In places where no preexisting oceanic sediments are trapped between igneous basement and the recent volcanic edifice to provide a mecanically weak layer, the latter is severely deformed. This gives further support to our interpretation of horizon V as being the base of the edifice and suggests that the top of the preexisting oceanic sediments is an active decollement, at least in the distal part of the edifice.

The nature of the substratum on which the volcanic edifice is built is considered as an important factor in models of volcano spreading [*Borgia*, 1994]. Analogue models developed by *Merle and Borgia* [1996] argue for deformation of a thick, ductile layer in the substratum; such models have been proposed for Hawaii [*Borgia et*

al., 1990; *Borgia and Treves*, 1992]. At La Réunion, the sediments we imaged in this survey between the volcaniclastic edifice and the top of the oceanic basement appear undeformed; hence the top of the oceanic plate may be a decoupling surface. This is supported by two lines of evidence: the lateral continuity and reverse polarity of reflector V (Figures 3 and 4), and the spatial correlation between basement highs and bathymetric bulges of intensely deformed parts of the apron (Figures 5 and 6).

4.2.2. Construction of the edifice. The relative geometry of intraedifice reflectors observed east of the island (Figure 10) has implications for models of edifice construction. The unit above discordance "h" is filling a preexisting depression in the lower portion of the edifice. Such localized bodies, discordant with respect to underlying reflectors, are observed in the eastern area of the survey. This may be due to the fact that their formation requires a relatively long history of mass wasting episodes to produce highs and lows that could be subsequently filled. However, the acquisition favored radial profiles, while termination of most of these intrapile reflections are observed on circular lines. Therefore other units with similar geometry may exist. An isopach map of the unit above h has been drawn taking a velocity of 3 km/s for the depth conversion and restricting its lateral extent to the "Ralé-Poussé" area, a zone of avalanche deposit identified by *Labazuy* [1991] (Figure 11). It gives a volume of at least 160 km^3, much larger than the 30 km^3 estimate based on morphological studies [*Labazuy*, 1991, p. 180; *Bachèlery et al.*, 1996].

The unit beneath horizon h may be more than the result of older landslide episodes. Near the northeastern shore of the island, a prominent magnetic anomaly of reverse polarity, interpreted as originating from material older than 0.7 Ma, provides evidence for remnants of an older volcano against which the Piton de la Fournaise has been built [*Malengreau*, 1995; J.-F. Lénat et al., unpublished manuscript, 1997]. The plutonic body drilled beneath the eastern flank of the Piton de la Fournaise [*Rançon et al.*, 1987] may be related to such early submarine volcanic activity, but the available potential field data do not permit it to be traced offshore [*Rousset et al.*, 1987]. Our seismic profiles also suggest that the growth and geometry of La Réunion are guided by earlier (submarine?) volcanic edifice(s).

5. Discussion of Vertical and Lateral Movements

The top of the oceanic basement "B" and the top of the preexisting oceanic plate "V" are two markers of the deformation related to hotspot emplacement and evolution. No other stratigraphic marker could be identified, except for horizons h and h', in the eastern part of the study area (Figures 10, 11, and 13). The absence of a peripheral moat and associated basement arch makes the seismic stratigraphy rather different from other volcanic edifices where seismic data are available, Hawaii and the Marquesas.

Flexural models have been proposed to explain both the Marquesas and Hawaiian moats and associated seismic patterns of onlap and offlap [*Watts and ten Brink*, 1989; *Wessel*, 1993; *Wolfe et al.*, 1994]. In La Réunion, prior to this study and in the absence of seismic data, a similar class of models has been invoked to explain geoid anomalies [*Bonneville et al.*, 1988]. The new data presented in this paper lead to a rather different view.

On most of the data, V does not appear as a distinctive and well-documented unconformity. This lack of angular unconformity in the volcano-sedimentary pile that covers the oceanic basement establishes the lack of significant vertical movement at a regional scale. This is at odds with Hawaii or the Marquesas volcanic edifices where fanning of the stratigraphic units is ubiquitous [*ten Brink and Watts*, 1985; *Wolfe et al.*, 1994].

Preexisting oceanic sediments are subparallel, but on a few profiles, the observed stratification is slightly tilted away from the island (Figure 6). This geometry suggests that the doming of the preexisting plate, inferred from both the MCS (this paper) and the wide-angle data [*Charvis et al.*, this issue], is a recent feature, related to hotspot magmatic activity. However, the short-wavelength basement topography revealed by this study clearly predates the hotspot influence and may be attributed to the complex Paleocene accretionary history.

Southwest of the island, two radial profiles, R22 and R23, shot parallel to each other and only 15 km apart, show a marked difference in depth to basement (Plate 1 and Figure 9). Near the shore, this change in the depth of the oceanic basement is constrained by the northwest-southeast line recorded on OBS 15 (located on Figure 2) to occur within 15 km on either side of that OBS [*Charvis et al.*, this issue]. This geometry indicates a structure trending SW-NE. It seems difficult to admit a chance coincidence of the position of the profiles to encompass a basement fault scarp. However, its azimuth, constrained by the direction of lines R22 and R23, happens to be in the direction of spreading at the age of seafloor formation; hence this structure could be a transform fault of this spreading system. From the study of magnetic lineations, a structural interpretation of the seafloor had been proposed by *Schlich* [1975] and revised by *Dyment* [1991]. It shows a dissection by closely spaced transform faults (Figure 1), one of which happens to coincide with the basement step revealed here.

Figure 9 implies that on profile R23, V coincides with a top discordance of the preexisting oceanic sediments (or upper sequence boundary) as defined by seismic stratigraphy [*Mitchum*, 1977]. This is observed only in the southern part of the survey area. A surprising result from the MCS data is the existence of a fault scarp, 40 m high, observed about 150 km southwest of the island, on the tie line between R22 and R23 (Fig-

ure 9). This fault displaces the seafloor sediments in an area where no recent tectonic activity was expected. On profile R22, we observe landward stepping of terminations in the most recent sediments, presumably contemporaneous with La Réunion volcanic activity; this is consistent with upward motion of the low-lying basement block east of this scarp but may also be related to variations in sediments influx. We interpret this fault as related to reactivation induced by hotspot activity of an older oceanic fracture zone.

Gravity implications of our interpretation are discussed by *Charvis et al.* [this issue], who conclude that there is <1 km plate flexure (if any) on the basis of the oceanic basement topography. More sophisticated modeling, taking into account dynamic compensation due to the presence of the thermal plume has not been done. The doming of the top of the preexisting plate documented by our seismic reflection data suggests that dynamic uplift may be of importance at La Réunion. This is quite different from the Hawaiian chain and not taken into account in the modeling of *Bonneville et al.* [1988]. A fractured lithosphere (Figure 9) with lateral rigidity variations is suggested by our data and also invoked by *Bonneville et al.* [1995] to explain their recent heat flow data.

The gentle overall doming of the top of the preexisting plate (Plate 1, top) will facilitate gravity sliding and slumping. There is no need to invoke forces coming from fluid push or volcanic loading, two mechanisms commonly invoked to explain geological observations [*Merle and Vendeville*, 1995]. Rift zones such as the ones documented offshore in Hawaii to a distance of 50 km [*Lonsdale*, 1989] are not observed. The northeast and southeast rift zones of the active volcano, inferred from surface geology [*Chevallier and Bachèlery*, 1981], do not extend at sea in any feature we could identify in this study. On land, the Fournaise rift zones do not correspond to high-velocity bodies [*Lankar-Bénichou*, 1997].

The effects of mass wasting processes are twofold: they carry material over large distance; they create relative highs and lows in the average bathymetry, or may even segment the apron. The resulting topography will affect the path of subsequent material transport. The data presented here show that mass wasting is largely episodic, though creep-like slumping may also exist.

6. Conclusions

A series of offshore seismic reflection profiles reveal the three-dimensional structure of the volcanic edifice of La Réunion hotspot. After careful processing that included prestack deconvolution, two stratigraphic markers of the deformation, the top of the oceanic basement and the top of the preexisting oceanic plate (i.e., the base of the volcaniclastic edifice), could be correlated on all profiles, with an average of 600 m of oceanic sediments in between. These results are summarized in isobath maps.

Significant three-dimensional variation of the topography of the oceanic basement is observed as a function of the direction to the island. A slight deepening, 1000 m at most, of the top of the basement toward the island is observed on its southwestern side. Elsewhere, either shallowing of the basement toward the island (northeastern side) or a complex topography with highs and lows is documented. Most of this topography is attributed to the complex accretionary history of the oceanic lithosphere in the study area.

The top of the preexisting oceanic plate does not show the regional depression expected from flexural models of island loads. No flexural moat and associated peripheral bulge comparable to the one flanking the Hawaiian Islands is observed around La Réunion. No evidence for flexure is found in the seismic stratigraphy. Doming instead of the expected flexure is observed near the island, with a control by and possible reactivation of Paleocene seafloor spreading features, notably an inferred fracture zone southwest of the island.

The total volume of the volcaniclastic edifice is estimated to be 75,000 km^3. This is significantly smaller than previous estimates which included a 4 km flexural depression, which was found to be nonexistent by our survey.

The submarine apron appears as a composite constructional body, resulting from alternating, discontinuous mass wasting episodes. Gravitational collapse induces lateral spreading by slumping of the flank of the edifice. Lateral transport is guided by preexisting topography. Landslides are documented south of the island, not only resulting from the active volcano Piton de la Fournaise on the eastern side. Several levels of decollement are suggested by our data, the top of the preexisting oceanic sediments being the deepest but not the only one.

Acknowledgments. Logistic and financial support during the MD76-REUSIS cruise was provided by IFRTP (Institut Français pour la Recherche et la Technologie Polaires), IFREMER (Institut Français de Recherche pour l'Exploitation de la Mer), and GENAVIR (Groupement pour la Gestion des Navires Océanologiques). Special thanks to the team that made the seismic acquisition successful: J. Hervéou, J. Le Pavec, R. Dereat, J.-C. Guedès, B. Meneur, O. Quedec, and D. Vaillant from IFREMER-GENAVIR; B. Ollivier and Y. Balut from IFRTP and the crew of the M/V *Marion Dusfrene*; all the colleagues of the MD76-REUSIS scientific party (M.D.P. Ayarza, L. Driad, Y. Hello, G. Lelong, S. Le Roux, W. O'Brien, S. Operto, B. Pontoise, L. Royer, M. Sachpazi, and B. Toussaint); and the representatives of the Mauritius Island Republic (P.O. Randamy, L. Joottun, and A. Sheik-Mamode). MCS data processing was carried out at the Geophysical Laboratory of the University of Pau mostly with ProMAX commercial software. Seismic Unix free software [*Cohen and Stockwell*, 1993] was used during the cruise. GMT free software [*Wessel and Smith*, 1995] was a great help in drawing the maps. We thank J-F. Lénat and P. Labazuy for their bathymetric data and for discussions, L. Fleitout for data on oceanic sediments, and A. Levander, J. McBride, and an anonymous reviewer for their comments. The REUSIS-FOURNASEIS project was funded by the European Community Volcanic Risk pro-

gramme under contract EV5V-CT92-0188. UMR 6526 contribution 213.

References

Bachèlery, P., P. Labazuy, and J.-F. Lénat, Avalanches de débris sous-marines et subaériennes à la Réunion, *C. R. Acad. Sci., Ser. D, 323,* 475-482, 1996.

Bassias, Y., M. Denis-Clocchiatti, and L. Leclaire, Le Plateau des Mascareignes: Evolution d'une plate-forme néritique en milieu océanique, *C. R. Acad. Sci., Ser. D, 317,* 507-514, 1993.

Bonneville, A., J.-P. Barriot, and R. Bayer, Evidence from geoid data of a hot spot origin from the southern Mascarene Plateau and Mascarene Islands (Indian Ocean), *J. Geophys. Res., 93,* 4199-4212, 1988.

Bonneville, A., et al., Une lithosphère amincie sous le point chaud de La Réunion? Contraintes apportées par de nouvelles mesures de flux de chaleur sur la ride des Mascareignes, *C. R. Acad. Sci., Ser. D, 321,* 909-915, 1995.

Borgia, A., Dynamic basis for volcanic spreading, *J. Geophys. Res., 99,* 17791-17804, 1994.

Borgia, A., and B. Treves, Volcanic plates overriding the ocean crust: structure and dynamics of Hawaiian volcanoes, in *Ophiolites and Their Modern Analogues,* edited by M.L. Parson, J.B. Murton, and P. Browning, *Geol. Soc. Spec. Publ. London, 60,* 277-299, 1992.

Borgia, A., J. Burr, W. Montero, L.D. Morales, and G.E. Alvarado, Fault propagation folds induced by gravitational failure and slumping of the central Costa Rica volcanic range: Implications for large terrestrial and Martian volcanic edifices, *J. Geophys. Res., 95,* 14357-14382, 1990.

Charvis, P., A. Laesanpura, J. Gallart, A. Hirn, J.-C. Lépine, B. de Voogd, T.A. Minshull, Y. Hello, and B. Pontoise, Spatial distribution of hotspot material added to the lithosphere under La Réunion from wide-angle seismic data, *J. Geophys. Res.,* this issue.

Chevallier, L., and P. Bachèlery, Evolution structurale du volcan actif du Piton de la Fournaise, Ile de la Réunion, Océan Indien Occidental *Bull. Volcanol., 44,* 723-741, 1981.

Cochonat, P., et al., Glissements et dépôts gravitaires en domaine volcano-sédimentaire sous-marin (volcan de la Fournaise, Ile de la Réunion, *C. R. Acad. Sci., Ser. II, 311,* 679-686, 1990.

Cohen, J.K., and J.W. Stockwell Jr., SU/CWP: Seismic Unix release 19, a free package for seismic research and processing; Cent. for Wave Phenomena, Colo. Sch. of Mines, Golden, 1993.

Denlinger, R.P., and P. Okubo, Structure of the mobile south flank of Kilauea volcano, Hawaii, *J. Geophys. Res., 100,* 24499-24507, 1995.

Duffield, W.A., L. Stieltjes, and J. Varet, Huge landslide blocks in the growth of Piton de la Fournaise, La Réunion, and Kilauea volcano, Hawaii, *J. Volcanol. Geotherm. Res., 12,* 147-160, 1982.

Duncan, R.A., J. Backman, and A. McDonald, Reunion hotspot activity through Tertiary time: Initial results from Ocean Drilling Program Leg 115, *J. Volcanol. Geotherm. Res., 36,* 193-198, 1989.

Dyment, J., Structure et évolution de la lithosphère océanique dans l'océan Indien: Apport des anomalies magnétiques. Ph.D. thesis, 374 pp., Univ. of Strasbourg, Strasbourg, France, 1991.

Gallart, J., L. Driad, P. Charvis, M. Sapin, A. Hirn, J. Diaz, B. de Voogd, and M. Sachpazi, Perturbation to the lithosphere along the hotspot track of La Réunion from an offshore-onshore seismic transect, *J. Geophys. Res.,* this issue.

Gillot, P.-Y., J.-C. Lefèvre, and P.-E. Nativel, Model for the structural evolution of the volcanoes of Réunion Island, *Earth Planet. Sci. Lett., 122,* 291-302, 1994.

Kent, G.M., I.I. Kim, A.J. Harding, R.S. Detrick, and J.A. Orcutt, Suppression of sea-floor- scattered energy using a dip-moveout approach-Application to the mid-ocean ridge environment, *Geophysics, 47,* 821-834, 1996.

Labazuy, P., Instabilités au cours de l'évolution d'un édifice volcanique, en domaine intraplaque océanique: Le Piton de la Fournaise (Ile de la Réunion), Ph.D. thesis, 260 pp., Univ. Clermont-Ferrand, Clermont-Ferrand, France, 1991.

Lankar-Bénichou, V., Approches en tomographie sismique du Piton de la Fournaise, Ph.D. thesis, Univ. of Paris 7, Paris, 1997.

Larner, K., R. Chambers, M. Yang, W. Lynn, and W. Wai, Coherent noise in marine seismic data, *Geophysics, 47,* 854-886, 1983.

Lénat, J.-F., Structure et dynamique internes d'un volcan basaltique intraplaque océanique: Le Piton de la Fournaise (Ile de la Réunion), Ph.D. thesis, Univ. Clermont-Ferrand II, Clermont-Ferrand, France, 1987.

Lénat, J.-F., and P. Labazuy, Morphologies et structures sous-marines de La Réunion, in *Le volcanisme de La Réunion,* edited by J.-F. Lénat, pp. 43-74, Centre de Recherches Volcanologiques, Clermont-Ferrand, France, 1990.

Lénat, J.-F., P. Bachèlery, A. Bonneville, A. Galdeano, P. Labazuy, D. Rousset, and P.M. Vincent, Structure and morphology of the submarine flank of an active volcano: Piton de la Fournaise (Réunion island, Indian Ocean), *Oceanol. Acta, Vol. Spec. 10,* 211- 224, 1990.

Lipman, P.W., J.P. Lockwood, R.T. Okamura, D.A. Swanson, and K.M. Yamashita, Ground deformation associated with the 1975 magnitude-7.2 earthquake and resulting changes in activity of Kilauea Volcano, Hawaii, *U.S. Geol. Surv. Prof. Pap., 1276,* 45 pp., 1985.

Lonsdale, P., A geomorphological reconnaissance of the submarine part of the East Rift Zone of Kilauea Volcano, Hawaii, *Bull. Volcanol., 51,* 123-144, 1989.

McDougall, I., The geochronology and evolution of the young oceanic island of Réunion, Indian Ocean, *Geochim. Cosmochim. Acta, 35,* 261-270, 1971.

Malengreau, B., Structure profonde de la Réunion d'après les données magnétiques et gravimétriques, Ph.D. thesis, 366 pp., Univ. Blaise Pascal, Clermont-Ferrand, France, 1995.

Merle, O., and B. Vendeville, Experimetal modelling of thin-skinned shortening around magmatic intrusions, *Bull. Volcanol., 57,* 33-43, 1995.

Merle, O., and A. Borgia, Scaled experiments of volcanic spreading, *J. Geophys. Res., 101,* 13805-13817, 1996.

Mitchum, R.M., Jr., Glossary of seismic stratigraphy, in *Seismic Stratigraphy-Applications to Hydrocarbon Exploration.* edited by C.E. Payton, *AAPG Mem. 26,* 205-212, 1977.

Moore, J.G., D.A. Clague, R.T. Holcomb, P.W. Lipman, W.R. Normark, and M.E. Torresan, Prodigious submarine landslides on the Hawaiian Ridge, *J. Geophys. Res., 94,* 17465-17484, 1989.

Moore, J.G., W.R. Normark, and R.T. Holcomb, Giant Hawaiian landslides, *Annu. Rev. Earth Planet. Sci., 22,* 119-144, 1994.

Parkes, G.E., A.M. Ziolkowski, A.M. Hatton, and T. Haugland, The signature of an air-gun array: Computation from near field measurements including interactions-Practical considerations, *Geophysics, 49,* 105-111, 1984.

Pou Palomé, S., Structure et évolution de l'édifice volcanique du point chaud de la Réunion: Traitement et interpré-

tation des profils de sismique réflexion de la campagne REUSIS, Ph.D. thesis, Univ. de Pau, Pau, France, 1997.

Rançon, J.P., P. Lerebour, and T. Auge, Mise en évidence par forage d'une chambre magmatique ancienne à l'aplomb de la zone orientale du Piton de la Fournaise (Ile de la Réunion), implications volcanologiques, *C. R. Acad. Sci., 304,* 55-60, 1987.

Rees, B.A., R.S. Detrick, and B.J. Coakley, Seismic stratigraphy of the Hawaiian flexural moat, *Geol. Soc. Am. Bull., 105,* 189-205, 1993.

Rousset, D., A. Bonneville, and J.-F. Lénat, Detailed gravity study of the offshore structure of Piton de la Fournaise volcano, La Réunion, *Bull. Volcanol., 49,* 713-722, 1987.

Safar, M.H., Efficient design of air-gun arrays, *Geophys. Prospect., 24,* 773-778, 1976a.

Safar, M.H., Single water gun far-field pressure signatures estimated from near-field measurements, *Geophysics, 50,* 257-261, 1976b.

Schlich, R., Structure et age de l'Océan Indien occidental, *Mem. Hors Ser. Soc. Geol. Fr., 6,* 102 pp., 1975.

Schlich, R., J. Dyment, and M. Munschy, Structure and age of the Mascarene and Madagascar basins, paper presented at *Colloque International sur le Volcanisme Intraplaque: Le Point Chaud de la Réunion,* Inst. de Phys. du Globe, Paris, 1990.

Stieltjes, L., and P. Moutou, A statistical and probabilistic study of the historic activity of Piton de la Fournaise, Réunion Island, Indian Ocean, *J. Volcanol. Geotherm. Res., 36,* 67-86, 1989.

ten Brink, U.S., and A.B. Watts, Seismic stratigraphy of the flexural moat flanking the Hawaiian Islands, *Nature, 317,* 421-424, 1985.

Varnes, D.J., Slope movement type and processes, in *Landslides, Analysis and Control, Spec. Rep. 176,* edited by R.L. Schuster and R.J. Krizek, pp. 11-33, Natl. Acad. of Sci. U.S.A., Washington, D.C., 1978.

Wallace, M.H., and P.T. Delaney, Deformation of Kilauea volcano during 1982 and 1983: A transition period, *J. Geophys. Res., 100,* 8201-8219, 1995.

Watts, A.B., and D.G. Masson, A giant landslide on the north flank of Tenerife, Canary Islands, *J. Geophys. Res., 100,* 24487-24498, 1995.

Watts, A.B., and U. ten Brink, Crustal structure, flexure, and subsidence history of the Hawaiian Islands, *J. Geophys. Res., 94,* 10473-10500, 1989.

Watts, A.B., U. ten Brink, P. Buhl, and T. Brocher, A multichannel seismic study of lithospheric flexure across the Hawaiian-Emperor seamount chain, *Nature, 315,* 105-111, 1985.

Watts, A.B., C. Pierce, J. Collier, R. Dalwood, J.P. Canales, and T.J. Henstock, A seismic study of lithospheric flexure in the vicinity of Tenerife, Canary Islands, *Earth Planet. Sci. Lett., 146,* 431-447, 1997.

Wessel, P., A reexamination of the flexural deformation beneath the Hawaiian Islands, *J. Geophys. Res., 98,* 12,177-12,190, 1993.

Wessel, P., and W.H.F. Smith, New version of the generic mapping tools released, *Eos Trans. AGU, 76,* 329, 1995.

Wolfe, C.J., M.K. McNutt, and R.S. Detrick, The Marquesas archipelagic apron: Seismic stratigraphy and implications for volcano growth, mass wasting, and crustal underplating, *J. Geophys. Res., 99,* 13591-13608, 1994.

Ziolkowski, A., The determination of the far-field signature of an interacting array of marine seismic sources from near-field measurements-Results from the Delft Air Gun Experiment, *First Break, 5,* 15-29, 1987.

Ziolkowski, A., G. Parkes, L. Hatton, and T. Haugland, The signature of an air gun array: Computation from near-field measurements including interactions, *Geophysics, 47,* 1413-1421, 1982.

P. Charvis, UMR Géosciences Azur, ORSTOM, BP 48, F-06235 Villefranche-sur-mer, France. (charvis@obs-vlfr.fr)

J. Dañobeitia and J. Gallart, Institut de Ciences de la Terra, CSIC, Sole i Sabaris s/n, E-08028 Barcelona, Spain.

B. de Voogd, S. Pou Palomé, H. Perroud, and D. Rousset, Laboratoire de Géophysique, Université de Pau et des Pays de l'Adour, F-64000 Pau, France. (beatrice.devoogd@univ-pau.fr)

A. Hirn, Laboratoire de Sismologie Expérimentale, Institut de Physique du Globe, Boite 89, 4 place Jussieu, F-75252 Paris cedex 05, France. (hirn@ipgp.jussieu.fr)

(Received October 13, 1997; revised July 13, 1998; accepted August 25, 1998.)